PHILOSOPHICAL MAGAZINE A, 1984, VOL. 49, No. 1, 81–93

Surface structure and energetics of multiply twinned particles

By L. D. MARKS†

Cavendish Laboratory, Madingley Road, Cambridge CB3 0HE, England

[Received 21 May 1982 and accepted 30 June 1983]

ABSTRACT

Experimental results from thermally annealed particles of silver and gold in the size range 10–50 nm show the presence of re-entrant surfaces on the decahedral multiply twinned particles (MTPs). A theoretical model is developed to explain these results based on the Wulff construction modified to include twin-boundaries. In addition to reproducing the re-entrant surfaces, the theory suggests that the total surface energy of the decahedral form is sandwiched between those of a single crystal and an icosahedral MTP. Consequently the stability of the decahedral particles (in a certain size range) relative to single crystals can now be explained. A useful perturbation modification is also outlined which enables qualitative comparisons of the surface energies to be made, and shows that the twin boundaries in MTPs limit the possible surface facets. Explicit shapes and energies are presented for two extreme models of the faceting. Finally, a model is outlined to justify the difference between the structures reported here and the more common decahedra and icosahedra—the standard forms are artefacts of the growth process; they are not the thermodynamically most stable structures.

§1. INTRODUCTION

In small f.c.c. metal particles there often occur non-crystallographic structures, the so-called multiply twinned particles or MTPs. First observed and analysed in detail during the early stages of epitaxial growth (Ino 1966, Ino and Ogawa 1967, Allpress and Sanders 1967), MTPs have since been found during electrolytic deposition (Disgurd, Maurin and Roberts 1976), in argon smokes (see, for example, Hayashi, Ohno, Shigeki and Uyeda 1977) and in heterogeneous catalysts (Marks and Howie 1979). At present it appears that MTPs can occur in all f.c.c. metals and in some related materials such as carbon and silicon.

The basic structure of these particles can be described as a collection of single-crystal tetrahedra, twin-related on their adjoining faces: 5 tetrahedra arranged symmetrically about an axis with D_{5h} point group symmetry to form a decahedron, and 20 in a three-dimensional configuration with I_h symmetry producing an icosahedron, as illustrated in fig. 1. Each unit in the decahedral particles‡ has two twin-boundaries, as against three in the icosahedral particles. As such, neither of these configurations is completely space filling, so it is necessary to incorporate some form of internal strain, either homogeneous (Ino 1969), inhomogeneous (de Wit 1972), as dislocations (Saito, Yatsuya, Mihama and Uyeda 1978, Marks and Howie 1979, Marks and Smith 1981) or a structural modification (Bagley 1965, Heinemann,

† Present address: Department of Physics, Arizona State University, Tempe, Arizona 85287, U.S.A.

‡ In this paper we refer to MTPs generally (when the fundamental units are more complicated than tetrahedra) as decahedral or icosahedral MTPs, abbreviated to Dh and Ic respectively. The terms icosahedron and decahedron are reserved for the geometric structures.

Fig. 1

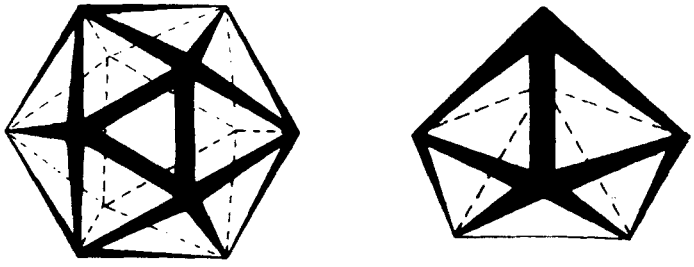

(a) (b)

Schematic diagrams of the structure of (a) icosahedral and (b) decahedral MTPs.

Yacaman, Yang and Poppa 1979, Yacaman, Heinemann, Yang and Poppa 1979, Yang 1979, Yang, Yacaman and Heinemann 1979). These elastic effects and the general energy balance between MTPs and single crystals will be discussed in a companion paper (Howie and Marks 1984).

An important problem with MTPs is their equilibrium surface morphology, a subject which is investigated here both experimentally and theoretically. In previous work (see, for example, Ino 1969, Allpress and Sanders 1970, Gordon, Cyrot-Lackman and Desjonqueres 1979) MTPs have been assumed to be perfect icosahedra or decadedra and the total surface energies obtained (for a given number of atoms) were in the order Dh > single crystal > Ic. (Ino (1969) added (100) facets to the Dh but still obtained the same ordering.) Arguing then that the total surface energy was more important than a detrimental strain energy in small particles, it was possible to justify the existence of very small Ics, but not Dhs. In this paper it is shown that the structure of thermally annealed Dhs is considerably more complicated, containing re-entrant surfaces at the twin boundaries. A theoretical model based on the Wulff construction (Wulff 1901) is developed which permits a general analysis of the surface thermodynamics of MTPs. Among other results, the total surface energies are now in the order single crystal > Dh > Ic, thereby removing the theoretical anomaly as to the cause of Dhs.

§2. Experimental procedure

Specimens of silver were prepared by evaporation in a vacuum of $< 2 \times 10^{-3}$ Pa onto amorphous carbon films at 500, 600 and 700°C, and air-cleaved NaCl at 500°C. These were then annealed at the deposition temperature for 30 min. A specimen of gold was prepared by evaporation under the same vacuum conditions on to amorphous carbon at 600°C, then annealed for 10 min. For both metals, a range of particle sizes was obtained by varying the deposition time across the substrates with a movable shutter. The specimens deposited on NaCl were prepared for electron microscopy by evaporation of a thin amorphous film over the particles, followed by transfer by water flotation of the film and particles on to microscope grids. The amorphous carbon substrates were premounted on microscope grids.

The particles prepared in this fashion were examined in a Siemens 102 electron microscope at 100 kV using axial bright-field imaging combined with either axial or hollow cone dark-field imaging with the (111) and (200) rings.

Fig. 2

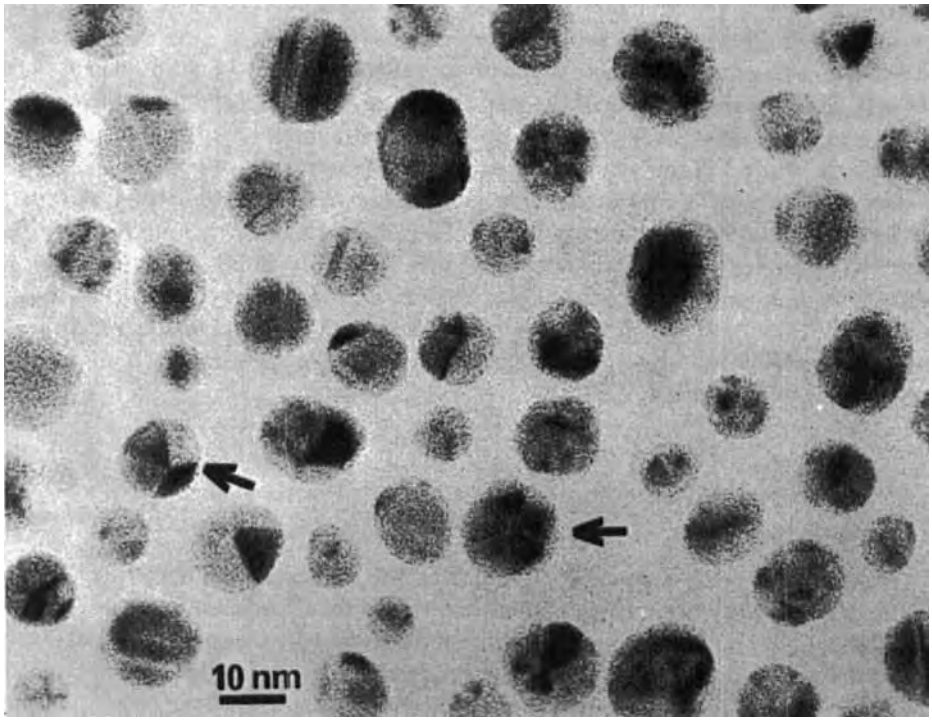

A typical field of view, here taken from a silver sample prepared on NaCl at 500°C. Two Dhs with the notches just visible are indicated.

Fig. 3

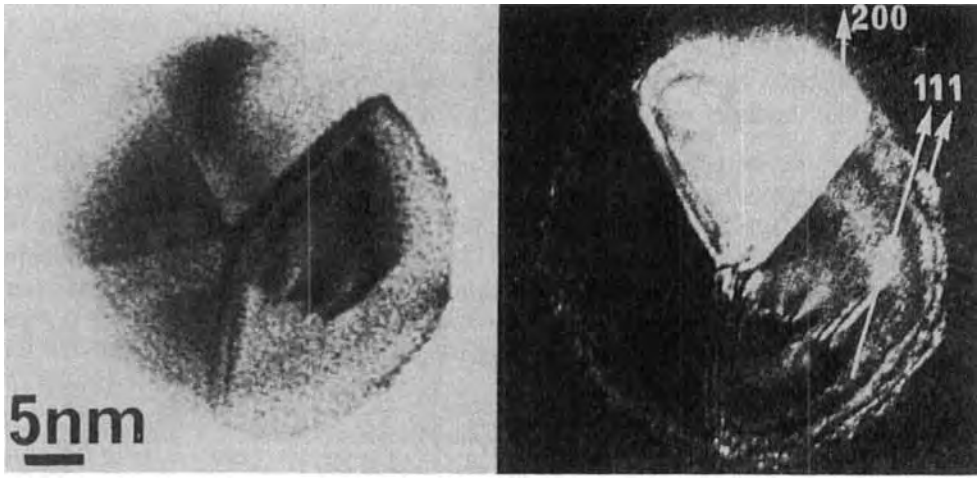

(*a*) (*b*)

A Dh of silver from the 700°C sample on amorphous carbon in (*a*) bright field and (*b*) dark field. The diffracted beams contributing to the image in (*b*) are indicated.

§3. Experimental results

A wide variety of particle types was observed, in agreement with previous work for similarly annealed particles (see, for example, Solliard, Buffat and Faes 1976, Takahashi, Suzuki, Kushima and Ogasaware 1978). A typical field of view is shown in fig. 2. The external profiles of the particles were rounded, crudely approximating to spheres, although facets could be distinguished at higher magnifications.

A particularly interesting result was the surface structure of the Dhs. Regardless of size, substrate or temperature, these particles possessed well-formed notches at the twin boundaries (as shown in fig. 3). The existence of these notches have been reported previously (Marks, Smith and Howie 1980), and similar effects at the twin boundaries have also been observed by Saito *et al.* (1978) and White, Baird, Fryer and Smith (1982). It can be seen from fig. 3 that the planes producing these re-entrant surfaces are nearly parallel to a nearby twin boundary, from which they were indexed as (111) facets.

§4. Theory

4.1. *Modified Wulff construction*

Here we deal with a model for predicting the arrangement of surface facets on MTPs. The theoretical problem is to minimize the total surface and twin-boundary energies of an assembly of single-crystal units at constant volume. Fortunately, it is not necessary to consider all the units simultaneously, as by the symmetry of the particles they are identical. Furthermore, this symmetry allows the twin boundaries to be partitioned into pairs of identical surface-like boundaries. Hence the problem reduces to one of minimizing the total surface energy of a single crystal with either two or three 'twin facets' (faces with an energy per unit area half that of a twin boundary) and a number of external surface facets.

This type of problem can be solved by using a Wulff construction (see, for example, Herring 1951). Describing the surface free energy in the functional form $\gamma_S(\theta, \phi)$, the solution is in three stages:

(1) draw $\gamma_S(\theta, \phi)$ in three dimensions as a polar plot,
(2) construct the planes normal to the radii at all points on $\gamma_S(\theta, \phi)$ and
(3) take the inner envelope of these planes.

The form of the construction for a single crystal is shown in fig. 4.

This same construction can be used for MTPs by including in $\gamma_S(\theta, \phi)$ extra point values of magnitude half that of the twin boundary per unit area ($\gamma_t/2$) in the appropriate $\langle 111 \rangle$ directions. Here we invoke the symmetry of the particles to halve the twin boundary, which is comparable to the approach taken by Cahn and Hoffman (1974). The construction is somewhat stronger than this, and can be used without this symmetry requirement, as discussed elswhere (Marks 1983).

4.2. *Perturbation approach*

The modified Wulff construction described above includes all the effects of the twin boundaries, but fails to provide any direct insight into the physical processes which determine the relative surface energies of MTPs and single crystals. For this it

Fig. 4

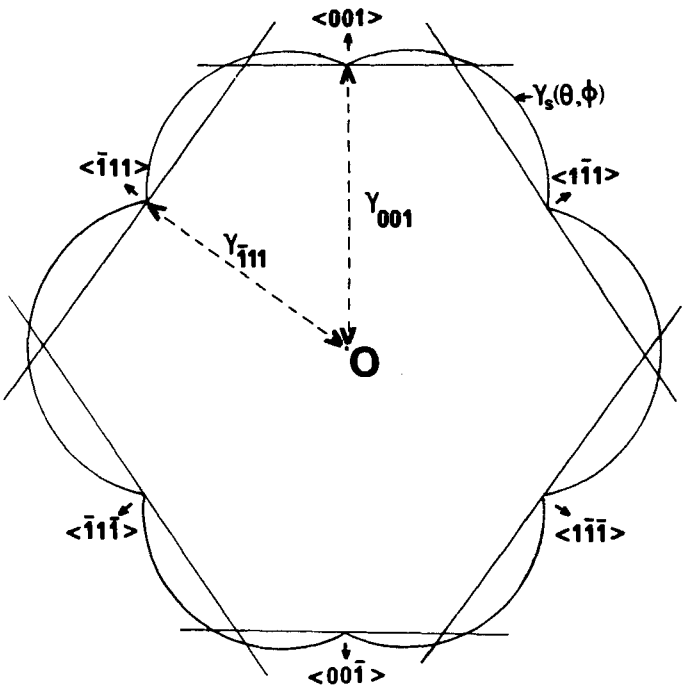

A ⟨110⟩ section through the Wulff construction for a single crystal under strong faceting conditions.

is better to treat the twin boundaries by perturbation theory. It is convenient to express the total surface energies by a dimensionless parameter

$$\varepsilon_\omega = \frac{1}{\gamma_{111}} \frac{\int \gamma_S(\theta,\phi)\, dS}{\left(\int dV\right)^{2/3}}, \tag{1}$$

where γ_{111} is the surface energy per unit area of a (111) facet. The advantage of using ε_ω is that it depends only on the particle shape and not on the volume. It is possible to expand ε_ω as

$$\varepsilon_\omega = \varepsilon_S + \frac{\gamma_t}{2\gamma_{111}}(\varepsilon_t + \varepsilon_c), \tag{2}$$

where ε_S is the zero-order term (obtained with $\gamma_t = 0$ in a modified Wulff construction), ε_t is the first-order term evaluated from the twin area of the $\gamma_t = 0$ construction, and ε_c is a twin-surface coupling term that includes all the higher-order terms. (A combination of ε_S and ε_t is similar to the treatment used by Ino (1969).)

For f.c.c. metals (except possibly aluminium and platinum) $\gamma_{111} \gg \gamma_t \approx 0{\cdot}01\gamma_{111}$, so ε_S is the dominant term in the energy. Examining the $\gamma_t = 0$ constructions, we find that the twin boundaries limit the possible surface facets. This effect is represented on the stereographic plot in fig. 5 (*a*), and a stereographic triangle divided into two angular domains A and B as shown in fig. 5 (*b*). The total regions shown in fig. 6 (*a*)

Fig. 5

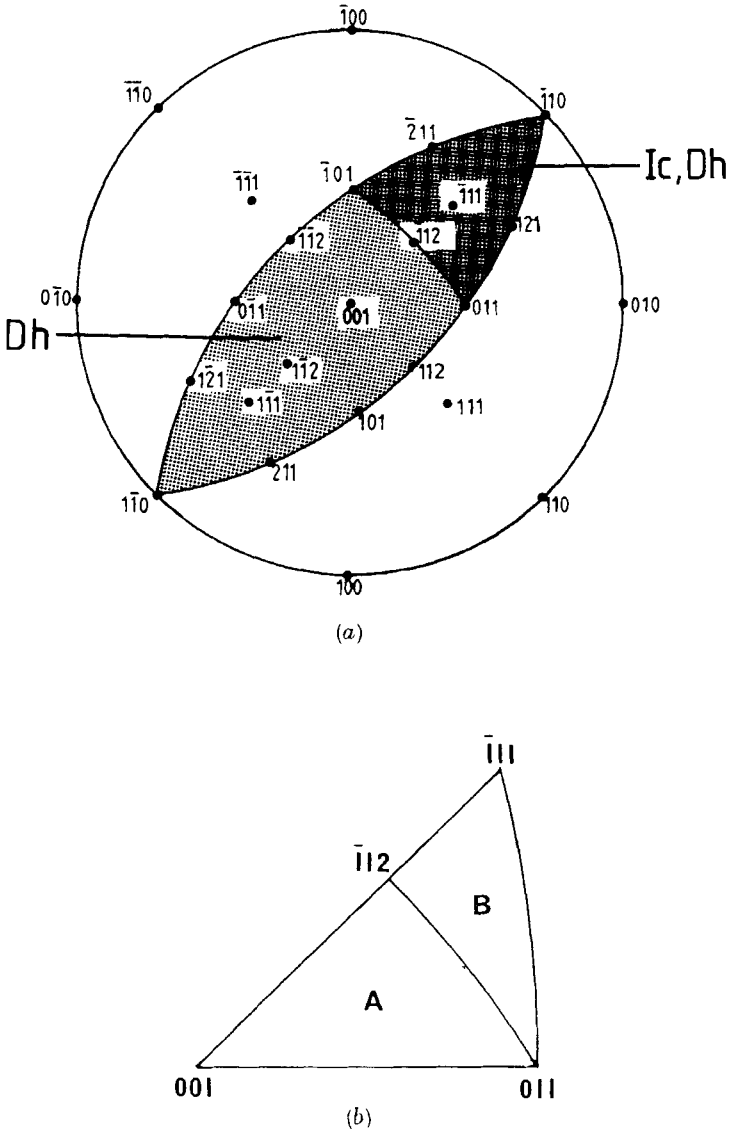

Stereographic diagrams for use with MTPs. In (*a*) the total shaded area describes the angular domain of a Dh unit, the darker area towards the top right indicating the domain of an Ic unit. The angular domains can be represented by suitable combinations of the two domains A and B shown in (*b*).

reduce so that a single crystal spans 48A and 48B domains, a Dh spans 40 A and 60 B domains, and an Ic spans 120 B domains.

Writing now for simplicity

$$\bar{\gamma}\Omega = \int \gamma_S(\theta, \phi)\, dS \tag{3}$$

for the integration over a solid angle Ω, we find that

$$\varepsilon_S = \left[\frac{9}{\gamma_{111}}(48\bar{\gamma}^A\Omega^A + 48\bar{\gamma}^B\Omega^B)\right]^{1/3} \tag{4}$$

for a single crystal,

$$\varepsilon_S = \left[\frac{9}{\gamma_{111}}(40\bar{\gamma}^A\Omega^A + 60\bar{\gamma}^B\Omega^B)\right]^{1/3} \tag{5}$$

for a Dh and

$$\varepsilon_S = \left[\frac{9}{\gamma_{111}}(120\bar{\gamma}^A\Omega^A)\right]^{1/3} \tag{6}$$

for an Ic. As $\Omega^A = 1{\cdot}6137\Omega^B$, then if

$$\bar{\gamma}^A > 0{\cdot}9296\bar{\gamma}^B \tag{7}$$

the total surface energies are qualitatively in the order single crystal > Dh > Ic.

Thus the relative surface energies of the different particle types depend solely on the relative surface energies of the two regions A and B.

§5. Theoretical results

The modified Wulff construction described above requires the form of $\gamma_S(\theta, \phi)$ to be known. Unfortunately, there is very little experimental evidence available for the low-temperature regime of interest. Therefore, two forms will be used here which represent the two extremes of faceting: a strong faceting model with (111) and (100) faces only (used already in fig. 4), and an isotropic model where $\gamma_S(\theta, \phi)$ is independent of direction.

5.1. *Strong faceting model*

The shape in this model of a single crystal (for reference), a Dh unit and an Ic unit are shown in figs. 6, 7 and 8, respectively. These were obtained by extracting the appropriate regions between the twin facets from the single crystal construction, as

Fig. 6

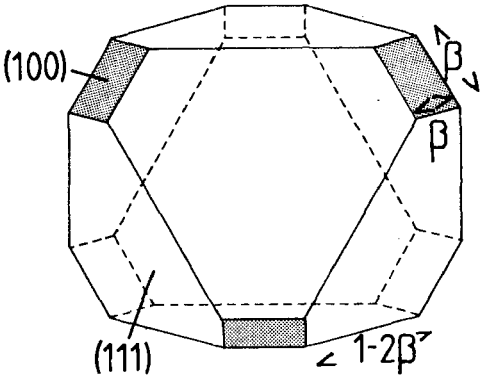

The shape of a single crystal in the strong faceting model.

Fig. 7

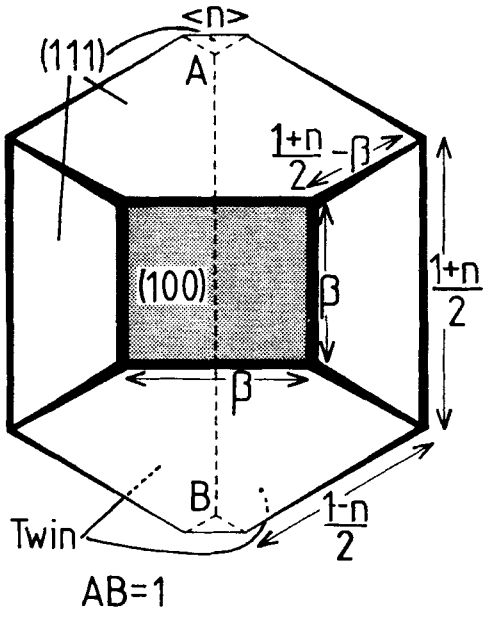

(a)

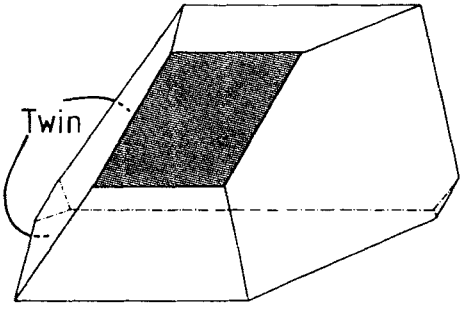

(b)

The structure of a Dh unit in the strong faceting model: (*a*) a plan diagram down the ⟨100⟩ direction, and (*b*) a 30° isometric. In both cases γ_t has been exaggerated for clarity.

illustrated for a Dh in fig. 9. All the shapes and the total surface energies given below are valid if

$$3\gamma_{111} \geq \sqrt{3}\gamma_{100} \geq \gamma_t, \tag{8}$$

which should in general be true for f.c.c. metals. (With a broken-bond model, $\gamma_{111} = (\sqrt{3}/2)\gamma_{100}$.)

The unit to be employed when building a Dh is considerably more complicated than a tetrahedron, possessing five additional facets. Two of these are very small, and are biproducts of the twin-surface coupling. It is unlikely that they will ever be present on experimental particles because of their size. For example, with a silver

Fig. 8

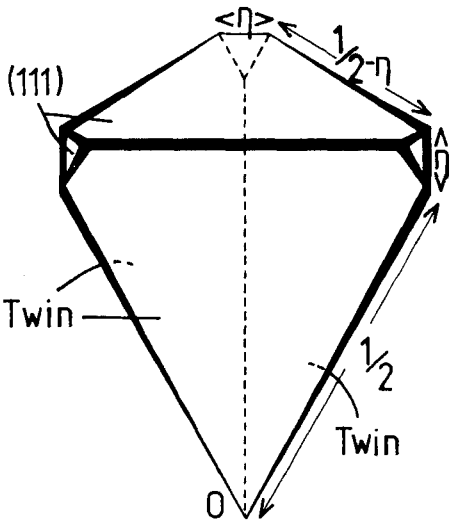

The unit for an Ic in the strong faceting model with γ_t exaggerated for clarity.

Fig. 9

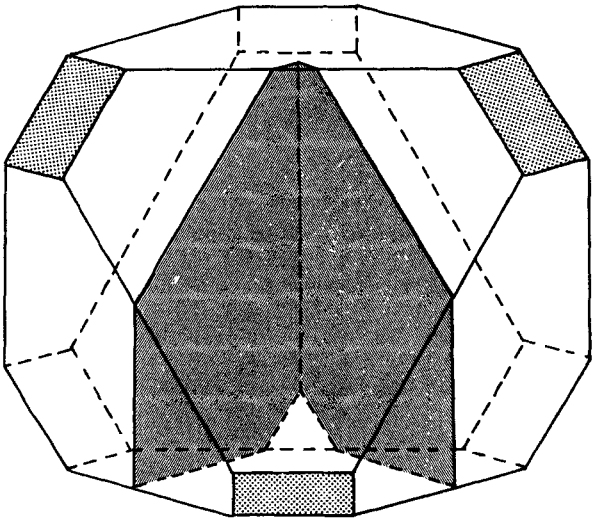

A complete modified Wulff construction for a strongly faceted Dh unit. The total shape is that of a single crystal, from which the appropriate areas are extracted by the twin facets (shaded).

particle of diameter 40 nm the side length of these facets is about 1 nm, i.e. the facet is equivalent to the loss of one atom. The other three facets, in contrast, are large, and lead to a generally more rounded shape with the experimentally observed notches at the twin boundaries (as illustrated with scale diagrams in fig. 10). A quantitative fitting to the experimental results could in principle be obtained with a value of

Fig. 10

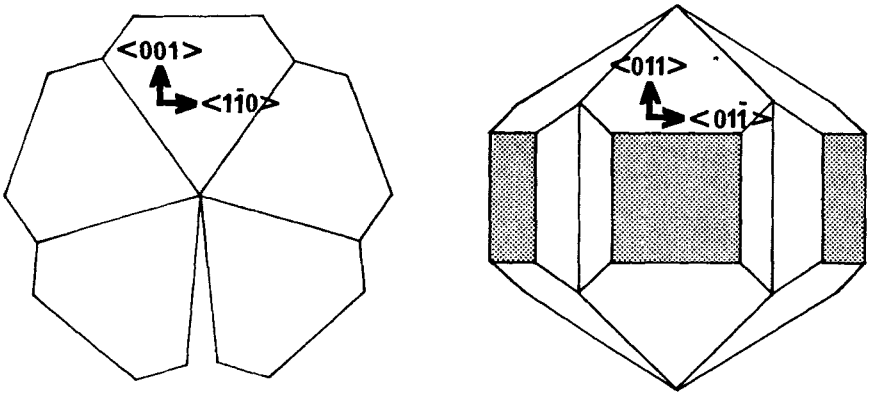

(*a*) (*b*)

Scale diagrams of a strongly faceted Dh for $\beta = 1/3$ and $\eta = 0{\cdot}005$. (*a*) $\langle 110 \rangle$ projection, (*b*) $\langle 100 \rangle$ projection (front surface only). The extra facets arising from twin-surface coupling have disappeared in the drafting. The similarity of (*a*) with tle particle shown in fig. 3 should be noted.

$\gamma_{100} = 2\gamma_{111}/\sqrt{3}$, and a few extra relatively small facets in the Wulff construction.

The unit for an Ic is by contrast almost exactly a tetrahedron. The only difference is the presence of three very small facets from the twin-surface coupling. However, the reservations outlined above for the similar facets present on the Dhs will apply here.

An important consequence of the new shape for the Dhs is that the total surface energy is now intermediate between those of single crystals and Ics. The various parameters for the Dhs are

$$\varepsilon_\omega = \{101\tfrac{1}{4}\sqrt{3}[(1+\eta)^3 - \tfrac{8}{3}(\beta^3+\eta^3)]\}^{1/3}, \tag{9}$$

$$\varepsilon_s = \{101\tfrac{1}{4}\sqrt{3}[1-(8\beta^3/3)]\}^{1/3}, \tag{10}$$

$$\varepsilon_t = \varepsilon_s/[1-(8\beta^3/3)], \tag{11}$$

so that

$$\varepsilon_w = \varepsilon_s\left[1+\frac{\eta}{1-(8\beta^3/3)}\right] - O(\eta^2), \tag{12}$$

where

$$\eta = \frac{\gamma_t}{2\gamma_{111}} \quad \text{and} \quad \beta = 1 - \frac{\gamma_{100}}{\sqrt{3}\gamma_{111}}. \tag{13}$$

These can be compared with

$$\varepsilon_\omega = \varepsilon_s = [108\sqrt{3}(1-3\beta^3)]^{1/3} \tag{14}$$

for a single crystal, and an Ic for which

$$\varepsilon_\omega = \{67\tfrac{1}{2}\sqrt{3}[(1+3\eta)^3 - 24\eta^3]\}^{1/3}, \tag{15}$$

$$\varepsilon_s = (67\tfrac{1}{2}\sqrt{3})^{1/3}, \tag{16}$$

$$\varepsilon_t = 3\varepsilon_s, \tag{17}$$

so that

$$\varepsilon_\omega = \varepsilon_s(1+3\eta) - O(\eta^2) \tag{18}$$

Explicit values for the various parameters are given in the table, evaluated for $\beta = 1/3$ (broken-bond model) and $\eta = 0{\cdot}005$ (a mean for f.c.c. metals).

Numerical values for the surface energy parameters, evaluated for $\beta = 1/3$ and $\gamma_t/2\gamma_{111} = \eta = 0{\cdot}005$.

Particle	ε_ω	ε_s	ε_t
Strong faceting model			
Decahedral MTP	5·436	5·407	5·999
Icosahedral MTP	4·899	4·890	14·670
Single crystal	5·499	5·499	—
Isotropic model			
Decahedral MTP	4·834	4·803	6·128
Icosahedral MTP	4·696	4·630	13·192
Single crystal	4·836	4·836	—

5.2. *Isotropic model*

With this form of $\gamma_s(\theta, \phi)$ a single crystal is a sphere, and the units for MTPs are regions of a sphere. For both terms of MTP, the external shape is, to a good approximation, spherical. For convenience, values of ε_s and ε_t are given rather than the complicated, full expressions for ε_ω.

The various energy parameters for an Ic are

$$\varepsilon_s = \{36\pi[1-(\Delta\Omega^{Ic}/4\pi)]\}^{1/3}, \tag{19}$$

$$\varepsilon_t = 5/2\varepsilon_s/[1-(\Delta\Omega^{Ic}/4\pi)], \tag{20}$$

$$\varepsilon_\omega = \varepsilon_s\left\{\frac{5\eta}{2[1-(\Delta\Omega^{Ic}/4\pi)]}\right\} - O(\eta^2), \tag{21}$$

and $\Delta\Omega^{Ic}/4\pi$ is the solid angle deficit in these particles given by

$$\frac{\Delta\Omega^{Ic}}{4\pi} = \frac{48\Omega^A - 72\Omega^B}{4\pi} = 1{\cdot}5405. \tag{22}$$

For a Dh the various values are:

$$\varepsilon_s = \{36\pi[1-(\Delta\Omega^{Dh}/4\pi)]\}^{1/3}, \tag{23}$$

$$\varepsilon_t = 5/4\varepsilon_s/(1-\Delta\Omega^{Dh}/4\pi), \tag{24}$$

$$\varepsilon_\omega = \varepsilon_s\left\{1+\frac{5\eta}{4[1-(\Delta\Omega^{Dh}/4\pi)]}\right\} - O(\eta^2) \tag{25}$$

and $\Delta\Omega^{Dh}/4\pi$, the solid angle deficit is given by

$$\frac{\Delta\Omega^{Dh}}{4\pi} = \frac{8\Omega^A - 12\Omega^B}{4\pi} = 0{\cdot}2568. \tag{26}$$

Finally, for a single crystal,

$$\varepsilon_\omega = \varepsilon_s = (36\pi)^{1/3}. \tag{27}$$

Explicit numerical values are given in the table, evaluated for $\eta = 0{\cdot}005$.

§6. Kinetic and thermodynamic surfaces

The major new experimental result that has been reported here is the totally new surface structure of the Dhs. As this is so different from the rather precise decahedra commonly reported, an explanation is required. The annealing appears to be responsible, as described below.

It is well established that early particulate growth occurs through the addition of an atom or a very small cluster to independent nuclei, with coalescence and secondary nucleation arising at a later stage (Pashley, Stowell, Jacobs and Law 1964). The occurrence of atomic growth when MTPs were present was confirmed by Allpress and Sanders (1967), while coalescence effects for these particles have been observed by Marks and Smith (1981). It is also known that atom-by-atom or layer growth is competitive, favouring the formation of low-index faces; the energy liberated when an atom adheres to a face is related to $-\gamma_s(\theta, \phi)$ so that high γ_s faces or favourable nucleation sites grow and are eliminated.

Therefore none of the faces with relatively high γ_s values which exist on the Wulff construction will be stable to the growth process. Furthermore, re-entrant surfaces such as those at the twin boundaries of the Dhs are known to be favourable nucleation sites (Frank 1949). The only stable facets will be the (111) facets not involved in the notches, as these will have the lowest γ_s values. Hence growth by the addition of individual atoms can be expected to produce decahedra and icosahedra, a prediction that would appear to be consistent with the previously reported structures.

It is only when the surfaces are equilibrated after growth has been completed that thermodynamic effects will become important. The type of process that one would expect is a gradual rounding of the particles on annealing, an effect which has in fact been observed by Takahasi *et al.* (1978), although this was attributed to contamination.

§7. Discussion

The agreement that has been obtained here between the experimental observations and the theoretical results would appear to be promising; rather surprising re-entrant surfaces on the thermally annealed Dhs are produced in the strong faceting model. Furthermore, the common observation of the rather precise icosahedra and decahedra forms would appear to be an artefact of these particles. The most significant characteristic of MTPs is the way in which the twin boundaries limit the types of face that can occur. Within this more generalized model, the Dhs occur in between single crystals and Ics, and may even be stable in their own right for certain particle sizes. (The question of the energy balance between MTPs and single crystals will be discussed more fully by Howie and Marks (1984).)

An important experimental question is the true form of $\gamma_s(\theta, \phi)$ at low temperatures, knowledge of which should allow the model to be tested more thoroughly. (Our experimental conditions were by no means sufficiently clean to allow any measurement of $\gamma_s(\theta, \phi)$ to be made from the particle morphologies,

beyond a qualitative fit.) Also of interest would be more information on the particle morphologies, particularly as a function of size. For example, the model can be expected to break down with very small particles when continuum assumptions become invalid; the unit cells of any high-index faces are large, so there may not be enough room for them to occur on MTPs below a certain size. Also of interest should be the effects of trace impurities or adsorbed gases, which may be strong as evidenced from both macroscopic experiments (see, for example, Flytzani-Stephanopoulous, Wong and Schmidt (1977) and ultra-high-vacuum studies (see, for example, Blakely and Somorjai 1977). Indeed, there would appear to be circumstantial evdience for a connection with important catalytic effects. Variations in the faceting might easily be a source of the known sensitivity of many heterogeneous catalysts to impurities.

Acknowledgments

The author would like to thank Drs. A. Howie and D. J. Smith for their extensive advice, and the U.K. SERC for financial support.

References

Allpress, J. G., and Sanders, J. V., 1967, *Surf. Sci.*, **7**, 1, 1970, *Aust. J. Phys.*, **23**, 23.
Bagley, B. G., 1965, *Nature, Lond.*, **208**, 674.
Blakely, D. W., and Somorjai, G. A., 1977, *Surf. Sci.*, **65**, 419.
Cahn, J. W., and Hoffman, D. W., 1974, *Acta metall.*, **22**, 1205.
de Wit, R., 1972, *J. Phys.* C, **5**, 529.
Disgurd, C., Maurin, M. G., and Roberts, J., 1976, *Met. Corres. Ind.*, **51**, 235, 320.
Flytzani-Stephanopoulous, M., Wong, S., and Schmidt, L. D., 1977, *J. Catal.*, **49**, 51.
Frank, F. C., 1949, *Discuss. Faraday Soc.*, **5**, 48, 186.
Gordon, M. B., Cyrot-Lackmann, F., and Desjonqueres, M. C., 1979, *Surf. Sci.*, **80**, 159.
Hayashi, T., Ohno, T., Shigeki, Y., and Uyeda, 1977, *Japan J. appl. Phys.*, **16**, 705.
Heinemann, K., Yacaman, M. J., Yang, C. Y., and Poppa, H., 1979, *J. Crystal Growth*, **47**, 177.
Herring, C., 1951, *Phys. Rev.*, **82**, 87.
Howie, A., and Marks, L. D., 1984, *Phil. Mag.* A, **49**, 95.
Ino, S, 1966, *J. phys. Soc. Japan*, **21**, 346; 1969, *Ibid.*, **27**, 941.
Ino, S., and Ogawa, T., 1967, *J. phys. Soc. Japan*, **22**, 1369.
Marks, L. D., 1983, *J. Crystal Growth*, **61**, 556.
Marks, L. D., and Howie, A., 1979, *Nature, Lond.*, **282**, 196.
Marks, L. D., and Smith, D. J., 1981, *J. Crystal Growth*, **54**, 425.
Marks, L. D., Smith, D. J., and Howie, A., 1980, *Electron Microscopy and Analysis 1979*, edited by T. Mulvey, Inst. Phys. Conf. Ser. No. 52 (London, Bristol: The Institute of Physica), pp. 397–400.
Pashley, D. W., Stowell, M. J., Jacobs, M. H., and Law, T. J., 1964, *Phil. Mag.*, **10**, 103, 127.
Saito, Y., Yatsuya, S., Mihama, K., and Uyeda, R., 1978, *Japan J. appl. Phys.*, **17**, 1149.
Solliard, C., Buffat, P., and Faes, F., 1976, *J. Crystal Growth*, **32**, 123.
Takahashi, M., Suzuki, T., Kushima, H., and Ogasaware, S., 1978, *Japan J. appl. Phys.*, **17**, 1499.
Yacaman, M. J., Heinemann, K., Yang, C. Y., and Poppa, H., 1979, *J. Crystal Growth*, **47**, 187.
Yang, C. Y., 1979, *J. Crystal Growth*, **47**, 274.
Yang, C. Y., Yacaman, M. J., and Heinemann, K., 1979, *J. Crystal Growth*, **47**, 284.
White, D., Baird, T., Fryer, J. R., and Smith, D. J., 1982, *Electron Microscopy and Analysis 1981*, edited by M. J. Goringe, Inst. Phys. Conf. Ser. No. 61 (London, Bristol: The Institute of Physics), p. 403.
Wulff, G., 1901, *Z. Kristallogr.*, **34**, 449.